In Situ Anomalous Small-Angle X-ray Scattering on an Operating Rechargeable Lithium Ion Battery Cell

A. Braun,[1] E. J. Cairns,[1] S. P. Cramer,[2] S. Seifert,[3] P. Thiyagarajan[4]

[1]*Lawrence Berkeley National Laboratory, Environmental Energy Technology Division, Berkeley, CA, U.S.A.*

[2]*Lawrence Berkeley National Laboratory, Physical Biosciences Division, Berkeley, CA , U.S.A.*

[3]*Argonne National Laboratory, CHM Division, Argonne, IL, U.S.A.*

[4]*Argonne National Laboratory, Intense Pulsed Neutron Source Division, Argonne, IL, U.S.A.*

Introduction

In the recent years, small-angle x-ray scattering was successfully applied in the study of electrode materials for supercapacitors.[1,2] batteries,[3] and fuel cells.[4] We now present results on the first *in situ* characterization of an operating lithium ion battery cell with X-ray absorption near-edge spectroscopy (XANES) and anomalous small angle X-ray scattering (ASAXS).[5] The cell contained $LiMn_2O_4$ spinel as a positive electrode and was charged and partially discharged. Contrast variation was applied to the manganese in order to study the evolution of microstructural changes in the electrode. A trimodal distribution of manganese containing objects was found. During electrochemical treatment, these objects grow by about 50%. Also, a reversible "flip" of a superstructure Bragg reflex was observed when the cell was fully charged.

Methods and Materials

Spinel and electrode were prepared as described in ref.[5] Electrode, Celgard® separator, LiPF6 electrolyte, and a lithium foil (125 µm thickness) were then assembled in an *in situ* cell (50% transmission at 6500 eV), which was sealed against contamination of electrodes with air and humidity. The cell was assembled in a helium filled glovebox, cabled to a portable potentiostat and data acquisition system and mounted at Advanced Photon Source beamline 12- ID, operated by the Basic Energy Sciences Synchrotron Radiation Center Collaborative Access Team. The cell was fully charged at very moderate currents of some 10 microamps and subsequently partially discharged. The cell voltage never increased 5 V. During electrochemical treatment, Mn K-edge XANES (7 min/spectrum) and ASAXS (0.1 sec/pattern) were recorded for 20 energies, which covered the Mn K-edge at 6545 eV and energies in its vicinity.

Results

Figure 1 displays three XANES spectra of the manganese in the electrode at three different stages of charge. Spectrum 1 (solid line) was obtained right at beginning of charging, with the electrode being LiMn2O4 and the open circuit potential 3.78 V. The manganese atoms per unit cell are present with the formal charges Mn4+ and Mn3+ in equal quantities. Spectrum 2 (broken line) was obtained when the cell was fully charged and most of the lithium in the spinel was removed, with a potential of 4.3 V. Spectrum 2 is shifted by about 1.5 eV towards higher energy, compared to spectrum 1. At this stage, the manganese is mostly (>90%) present as Mn^{4+}. At discharging (spectrum 3, dotted line), lithium is reinserted in the oxide lattice, and consequently the Mn is reduced. Thus,

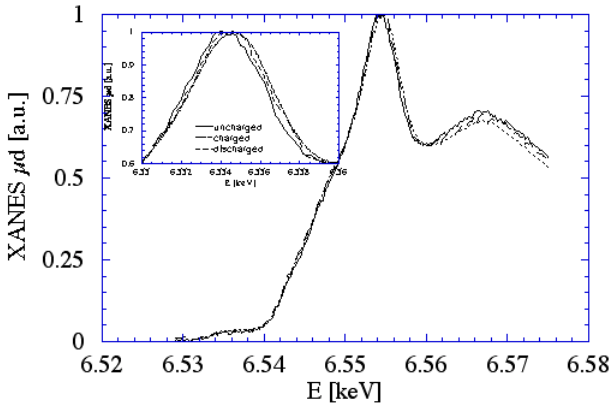

FIG. 1. Manganese K-edge XANES taken at 3 different stages of lithium concentrations (1-c): c=1 - uncharged, c=0 - charged, c=0.2 at discharge.

spectrum 3 is shifted towards a slightly smaller energy than spectrum 2. The potential was 4.05 V. The changes in the XANES serve as a verification of the valence changes of the manganese. The total charge and the lithium concentration were determined by integration of the current that passed through the cell.

Figure 2 shows ASAXS scattering curves (SC) of the electrode, which correspond to the above mentioned XANES spectra in terms of potential and Li concentration. Contrast variation was applied by the weighted difference of SC taken at 6400 eV (far below Mn K edge) and 6545 eV (right at Mn absorption edge). The SC shown in figure 2 have received the proper background subtractions. Significant humps in the intensity were found in the SC, which were subsequently treated in the Guinier approxima-

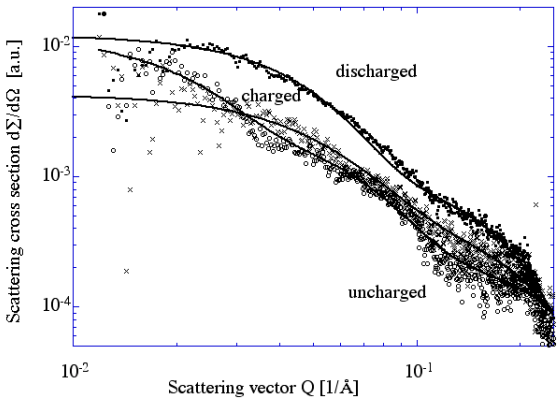

FIG. 2. ASAXS curves of samples corresponding to the state of charge as in Figure 1. Open circles: uncharged; crosses: charged; closed circles: discharged. The drawn lines represent least square bimodal Guinier fits.

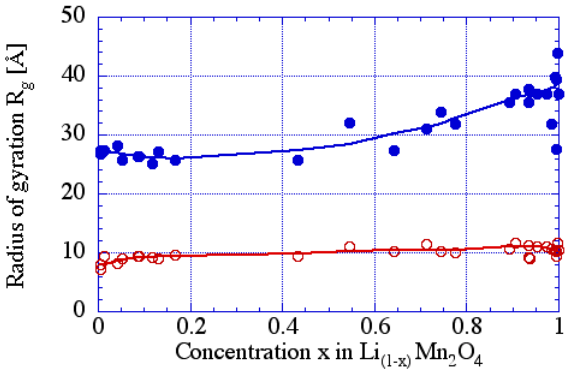

FIG. 3: Evolution of object-size as a function of concentration, as obtained from bimodal Guinier-Fits.

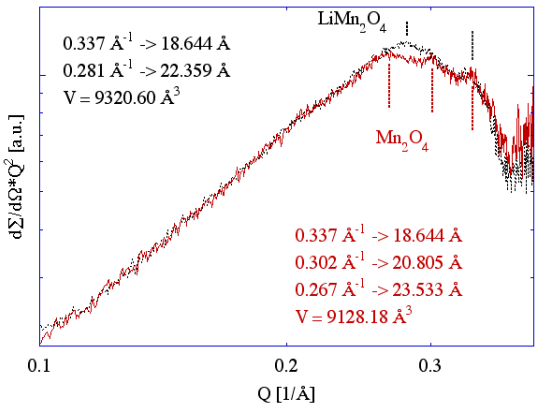

FIG. 4: Bragg-reflections of superstructure in Kratky-plot.

tion. Thirty-five sets of SC were analyzed over the whole range of Li concentration (1>c>0) during electrochemical cycling.

Within the Q-range under investigation (0.01<Q<0.2 1/Å), a trimodal distribution of manganese containing objects is found. Figure 3 shows the evolution of radius of gyration for the two smallest ranges of object size.

The manganese agglomerations in the oxid matrix grow from 7 Å to about 12 Å and from 25 Å to about 45 Å. These changes are irreversible.

Figure 4 shows the SC of the uncharged and charged samples in a Kratky-plot. We found this representation most suitable to show intensity peaks, which we assign to Bragg reflexions, probably reflecting an overstructure.[9] These weak peaks remain unchanged so far during cycling, with the exception of a major peak that shifted towards lower Q values right at the stage when the cell was fully charged. This “flip” of reflex was reversible, since it shifted back to its previouus position right after the onset of discharging. Among 35 studied SC, only this one, recorded at the moment of full charge and in line with the XANES showing the cell fully charged, showed the described anomaly. Since this effect appeared in a critically narrow window of concentration, it could be interpreted as a phase transition.

Discussion

Recently, microstructural changes in LiMn2O4 electrodes have been reported by various groups,[6-10] including the formation of nanometer-sized antiphase-domains, superstructures, phase transitions, and phase decompositions. The XANES and ASAXS data show that microstructural changes in lithium ion battery cells can be monitored *in situ* with these techniques. These changes occur in the spinel during (de-) lithiation even within the very first cycle at moderate currents in a safe potential range. The data obtained by Guinier analysis are probably not accurate, since the Guinier approximation is exact only to dilute systems, unless an interference function is taken into account. Therefore, the apparent Guinier radii are probably suppressed and underestimated due to interparticle interferences. Doubtless is the trend that the particles are growing during charging. This is confirmed by the monotoneous increase of the overall scattered intensity and scattering at zero angle, which is not plotted it in this report. Due to limited beam time and a pronounced careful charging of the cell, no time was left to measure the sample at smaller Q values and thus to resolve larger objects. We will continue these measurements and support them with additional x-ray diffraction experiments.

Acknowledgments

We are grateful to Erik Granlund (UC Berkeley Machine Shop) for manufacturing the *in situ* cell and Michael M. Thackeray and Christopher Johnson (ANL-CMT) for kind support with lithium and electrolyte on-site. Use of the Advanced Photon Source was supported by the U.S. Department of Energy, Basic Energy Sciences, Office of Science, under Contract No. W-31-109-Eng-38.

References

[1] A. Braun, M. Bärtsch, B. Schnyder, R. Kötz, O. Haas, H.-G. Haubold, G. Goerigk, J. Non-Cryst. Sol. **260** (1-2), 1-14 (1999).

[2] A. Braun et al., New Materials for Batteries and Fuel Cells, Mat. Res. Soc. Symp. Proc. Vol. **575**. pp. 369 (2000).

[3] W. Xing, J.S. Xue, T. Zheng, A. Gibaud, J.R. Dahn, J. Electrochem. Soc., **143** (11), 3482-3491 (1996).

[4] H.-G. Haubold, X.H. Wang, H. Jungbluth, G. Goerigk, and W. Schilling, J. Mol. Struc., **383** (1-3), 283-5 (1995).

5 A. Braun, S. Seifert, P. Thiyagarajan, S.P. Cramer, E.J. Cairns, accepted for publication in Electrochemixtry Communications.

[6] M.M. Thackeray et al., Electrochem. Solid-State Letters **1** (1) 7-9 (1998).

[7] M.M. Thackeray, W.I.F. David, P.G.Bruce, J.B. Goodenough, Mater.Res.Bull. **18**, 461 (1983).

[8] H. Wang, Y.-I. Jang, Y.-M. Chiang, Electrochem. Solid-State Letters **2** (10) 490-493 (1999).

[9] K. Kanamura, H. Naito, T. Yao, Z.-i. Takehara, J.Mater.Chem. **6** (1) 33-36 (1996).

[10] G. Rousse, C. Masquelier, R. Rodrigues-Carvajal, M. Hervieu, Electrochem. Solid-State Letters **2** (1) 6-8 (1999).